Solution-Processed Single-Emissive-Layer WOLEDs with High Efficiency and Ultra-High Color Rendering Index Beyond 90

Dongling Zhou,† Gang Cheng,†* Weiqiang Liu, Siping Wu and Chi-Ming Che*

Supporting Information

1. General experimental section:

OTPD, PYD2, DBP, DPEPO, TPBi and LiF were purchased from Luminescence Technology Corp, PEDOT: PSS from Heraeus. All of these materials were used as received without further purification. Emitters **Au-1**,[1] **Au-7**,[2] and **Au-8**[2] were synthesized according to reported procedures. The HOMO/LUMO energy levels of Au(III) complexes were estimated based on the formula of $E_{HOMO/LUMO} = -[4.8 + (E_{onset}^{ox/red}$ *versus* ferrocene $E_{1/2})]$ eV. The redox potentials of gold(III) complexes in *N*,*N*-dimethylformamide were recorded with 0.1 mol dm^{-3} $[n Bu_4N]PF_6$ as supporting electrolyte and saturated calomel electrode (SCE) as the reference electrode.[1-2]

The procedure for the preparation of thin-film samples for PL studies is described as follows: the mixture of PYD2 and dopant(s) in chlorobenzene (10 mg mL^{-1}) was spin coated on quartz films (1 × 1 cm) at a speed of 500 rpm inside a glove box and transparent film samples were obtained after being annealed at 70℃ for 20 minutes. Emission quantum yields of these thin-film samples were measured with Hamamatsu C11347 Quantaurus-QY Absolute PL quantum yields measurement system under argon atmosphere. Emission spectra of these thin-film samples were recorded on a Horiba

Fluorolog-3 spectrophotometer. The emission lifetime measurements were performed on a LP920-KS Laser Flash Photolysis spectrophotometer (Edinburgh Instrument Ltd.) equipped with a Q-switched Nd:YAG laser. The procedure for the preparation of thin-film samples for AFM measurement is described as follows: the mixture of PYD2 and dopant(s) in chlorobenzene (10 mg mL^{-1}) was spin coated on quartz slides covered by PEDOT: PSS at a speed of 3000 rpm inside a glove box and the transparent thin films were obtained after being annealed at 70℃ for 20 minutes. The prepared films were examined by atomic force microscope (AFM) with tapping mode (Bruker Nano Wizard ULTRA Speed 2).

Characterization data of **Au-1**, **Au-7**, and **Au-8**:

For **Au-1**, ^{1}H NMR (500 MHz, CD_2Cl_2): δ/ppm = 7.45 (d, *J* = 8.5 Hz, 2H), 7.27 (t, *J* = 8.5 Hz, 4H), 7.14 (d, *J* = 8.0 Hz, 4H), 7.07–7.04 (m, 4H), 7.00 (t, *J* = 7.5 Hz, 2H), 6.92 (dd, *J* = 2.5, 7.5 Hz, 2H), 6.66–6.61 (m, 2H), 3.16 (s, 6H); ^{19}F NMR (470 MHz, CD_2Cl_2): δ/ppm = -109.4, -111.6; ^{13}C NMR (150 MHz, CD_2Cl_2): δ/ppm = 170.45, 164.03 (dd, *J* = 10.5, 256.9 Hz), 161.70 (dd, *J* = 10.5, 259.5 Hz), 158.72 (d, *J* = 6.2 Hz), 158.04, 148.59, 145.04, 143.00, 134.62, 133.77, 129.51, 126.07, 124.03, 122.53, 117.81 (d, *J* = 20.0 Hz), 102.81 (d, *J* = 19.4 Hz), 102.50 (t, *J* = 26.5 Hz), 40.10; MS (FAB): m/z 785.2939 (M+); Elemental analysis calculated (%) for $C_{37}H_{26}AuF_4N_3$: C, 56.57; H, 3.34; N, 5.35; found: C, 57.04; H, 3.28; N, 5.29.

For **Au-7**, ^{1}H NMR (400 MHz, CD_2Cl_2): δ/ppm = 8.83 (s, 2H), 8.22 (d, *J* = 2.0 Hz, 2H), 7.67 (d, *J* = 8.2 Hz, 2H), 7.36 (dd, *J* = 8.2, 2.0 Hz, 2H), 7.29–7.25 (m, 4H), 7.10 (d, *J* = 7.5 Hz, 4H), 7.03 (t, *J* = 7.3, 2H), 6.82 (s, 2H), 2.61 (s, 6H), 1.36 (s, 18H); ^{13}C NMR (126 MHz, CD_2Cl_2): δ/ppm = 168.53, 157.92, 157.16, 148.32, 146.67, 144.88, 141.86, 138.85, 134.98, 129.76, 126.00, 125.01, 124.54, 123.35, 122.41, 120.76, 99.23, 98.30, 36.07, 31.55, 22.67; IR(KBr): ν = 2137 cm^{-1} (ν(C≡C)); MS(MALDI): m/z 835.3104 (M+); Elemental analysis calculated (%) for $C_{46}H_{44}AuN_3$: C, 66.10; H, 5.31; N, 5.03; found: C, 65.91; H, 5.36; N, 4.85.

For **Au-8**, ^{1}H NMR (500 MHz, CD_2Cl_2): δ/ppm = 8.83 (s, 2H), 8.19 (d, *J* = 2.0 Hz, 2H), 7.81 (d, *J* = 8.5 Hz, 2H), 7.67 (d, *J* = 8.5 Hz, 2H), 7.38 (dd, *J* = 8.5, 2.0 Hz, 2H), 7.34 (d, *J* = 8.5 Hz, 2H), 6.69–6.61 (m, 6H), 6.03–6.01 (m, 2H), 1.41 (s, 18H); ^{13}C NMR (126 MHz, CD_2Cl_2): δ/ppm = 168.23, 157.89, 157.02, 144.69, 144.35, 138.77, 138.09, 134.85, 134.73, 134.21, 131.09, 127.19, 125.92, 124.68, 123.72, 121.71, 115.67, 113.77, 101.26, 93.56, 35.86, 31.30; IR(KBr): ν = 2154 cm^{-1} (ν(C≡C)); MS(MALDI): m/z 821.2573 (M+); Elemental analysis calculated (%) for $C_{44}H_{38}AuN_3O \cdot 0.5CH_2Cl_2$: C, 61.84; H, 4.55; N, 4.86; found: C, 61.55; H, 4.47; N, 4.82.

Estimation of Förster radius:[3]

The Förster distance (R_{FRET}) is commonly utilized to evaluate the efficiency of a FRET process and can be expressed as the following equation:

$$(R_{FRET})^6 = \phi_D \kappa^2 \left(\frac{9000(\ln 10)}{128\pi^5 N_A n^4}\right) \int_0^\infty F_D(\lambda)\varepsilon_A(\lambda)\lambda^4 d\lambda \qquad (\text{in } Å^6)$$

where Φ_D is the emission quantum yield of the donor in the absence of the acceptor, and κ^2 is usually taken as 2/3 which is appropriate for dynamic random averaging of the donor and acceptor. n is the refractive index, whose value is taken as 1.49 for PMMA and 1.7 for other host materials. $F_D(\lambda)$ stands for the normalized emission spectrum of donor. $\varepsilon_A(\lambda)$ and N_A are the molar absorptivity of the acceptor and the Avogadro's number, respectively.

2. Fabrication and characterization of OLEDs:

An aqueous solution of PEDOT:PSS was spin-coated onto a cleaned ITO coated glass substrate and baked at 120 ℃ for 20 minutes to remove the residual water solvent in a clean room. The cross-linkable OTPD in toluene was spin-casted on top of the PEDOT:PSS layer and heated at 200 ℃ for 30 minutes to carry out cross-linking inside a N_2-filled glove box. The cross-linked OTPD was then subjected three times to a spin-

casted chlorobenzene solvent to remove the unreacted moieties. Afterwards, the mixture of PYD2 and emitting dopant(s) in chlorobenzene was spin-coated atop the OTPD layer inside the glove box. After being annealed at 70 ℃ for 30 minutes, all devices were subsequently transferred into a Kurt J. Lesker SPECTROS vacuum deposition system without exposure to air. In the vacuum chamber, organic materials of DPEPO and TPBi were thermally deposited in sequence at a rate of ~0.1 nm s^{-1}. Finally, LiF (1.2 nm) and Al (100 nm) were thermally deposited at rates of 0.03 and 0.2 nm s^{-1}, respectively.

EL spectra, CIE coordinates, CRI, CRI R_9, luminance-current-voltage characteristics, current efficiency, power efficiency and EQE were measured using a Keithley 2400 source-meter and an absolute external quantum efficiency measurement system (C9920-12, Hamamatsu Photonics). All devices were characterized at room temperature in ambient air environment without encapsulation. The efficiency roll-offs were evaluated based on the formula of $[(EQE_{max} - EQE_{1000}) / EQE_{max}]\times100\%$, in which EQE_{max} and EQE_{1000} refer to maximum EQE and EQE at a luminance of 1000 cd m^{-2} respectively.

Structural drawings of other supportive materials used in OLED fabrication:

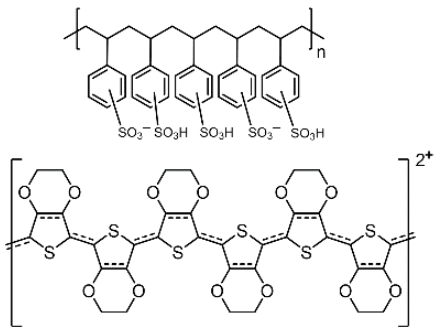

PEDOT:PSS

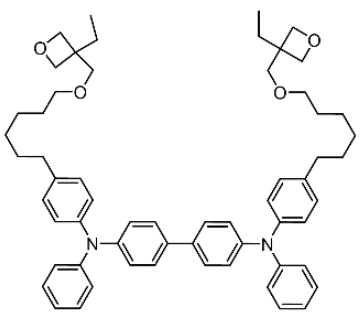

OTPD

3. Additional data:

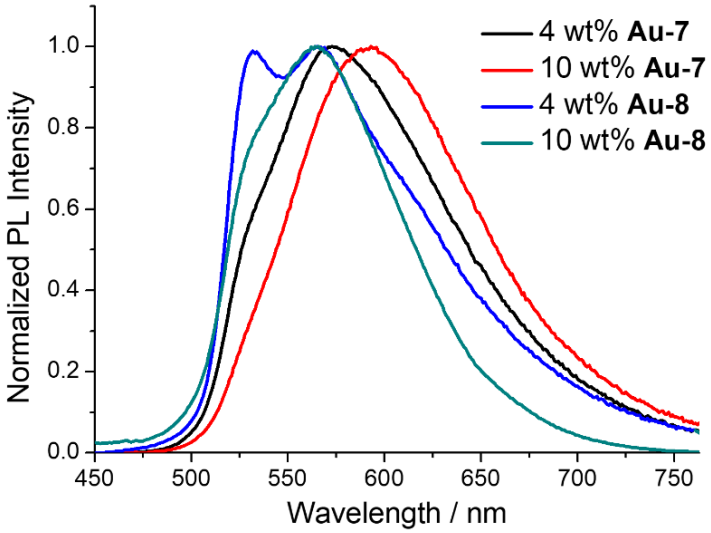

Figure S1. Normalized PL spectra of **Au-7** and **Au-8** doped in PYD2 thin films at different doping concentrations.

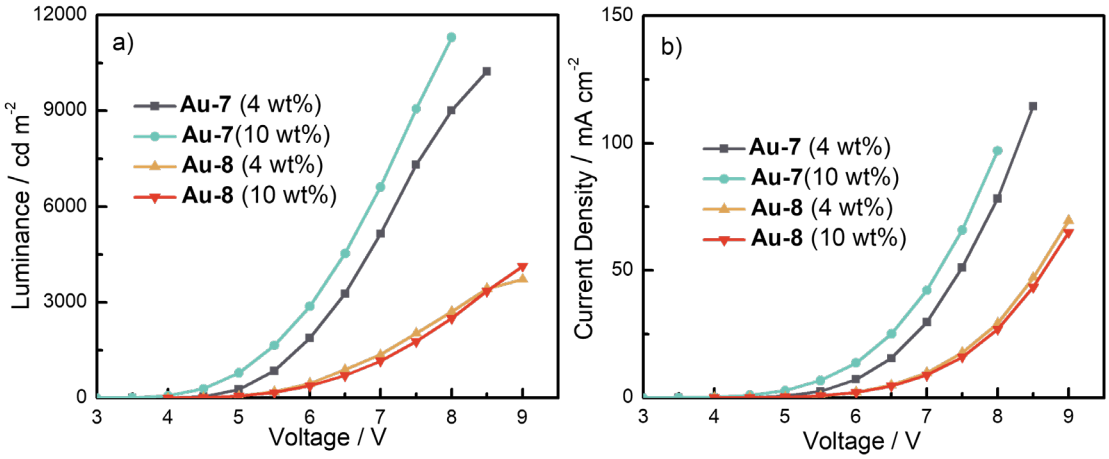

Figure S2. a) Luminance−voltage and b) current density−voltage characteristics of SP-OLEDs based on **Au-7** or **Au-8** at different doping concentrations.

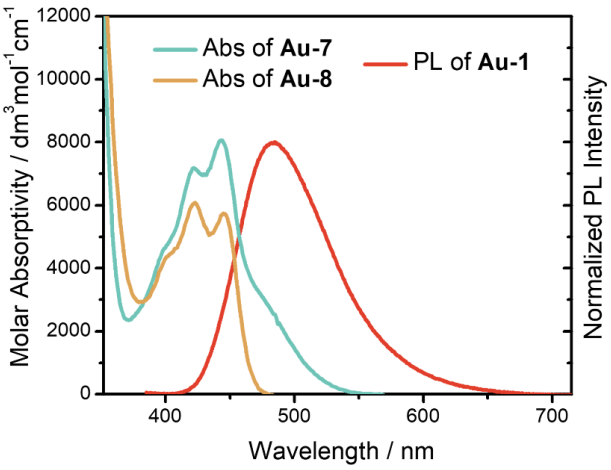

Figure S3. Absorption spectra of **Au-7** and **Au-8** in toluene solution (2×10^{-5} mol dm^{-3}) and emission spectrum of **Au-1** (4 wt%) doped in PMMA thin film. [The overlap of the emission spectrum of **Au-1** and the absorption spectrum of **Au-7** gives a spectral integral $J(\lambda)$ of 7.81×10^{13} M^{-1} cm^{-1} nm^4, while the spectral overlap between **Au-1** and **Au-8** affords a spectral integral $J(\lambda)$ of 1.45×10^{13} M^{-1} cm^{-1} nm^4.]

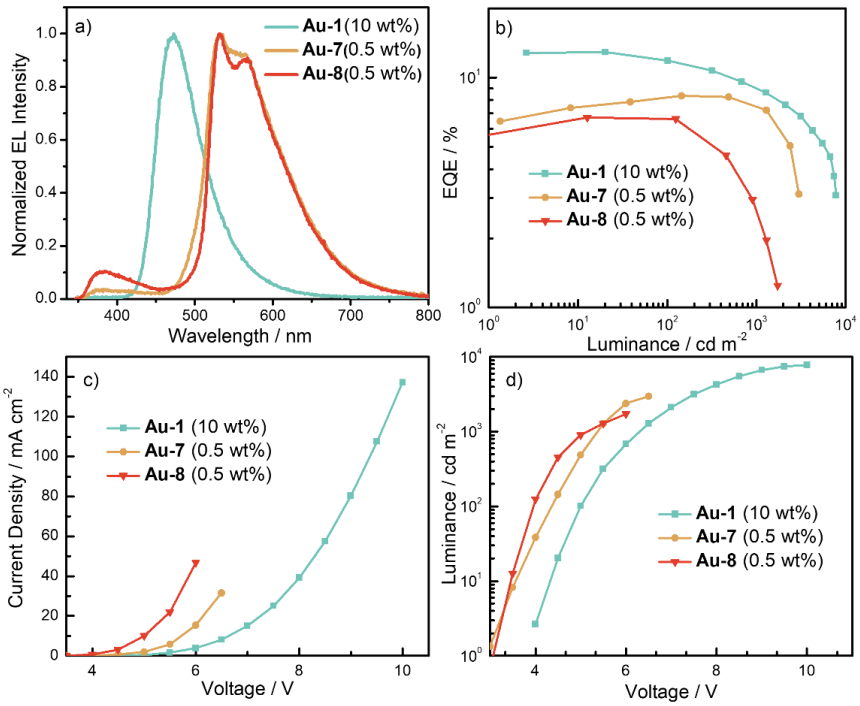

Figure S4. a) Normalized EL spectra, b) EQE−luminance, c) current density−voltage and d) luminance−voltage characteristics of devices based on **Au-1** (10 wt%), **Au-7** (0.5 wt%) or **Au-8** (0.5 wt%). [In the EL spectra of devices based on 0.5 wt% **Au-7** or **Au-8**, the emission at 380 nm stems from the PYD2 host.]

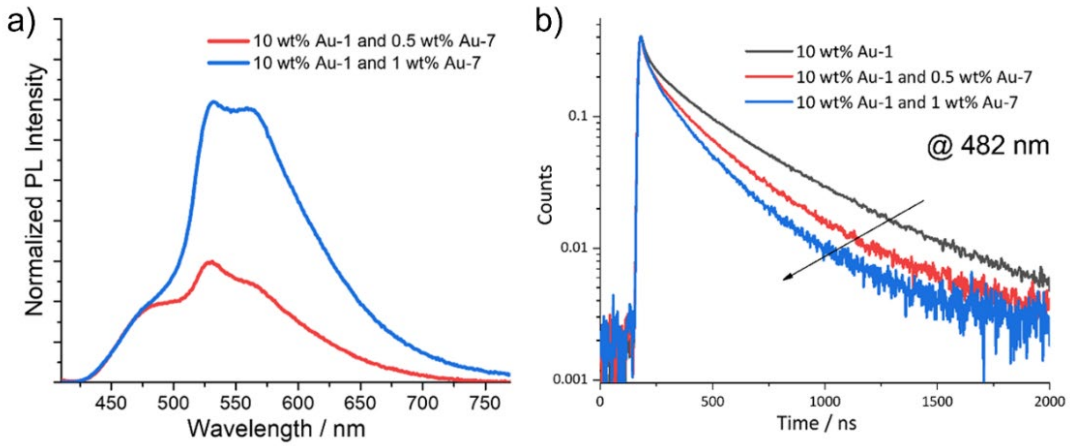

Figure S5. a) Emission spectra and b) PL decay curves of PYD2 thin films doped with different blend ratios of **Au-1** and **Au-7**. (The decay curves were measured at 482 nm under air). The lifetimes of the 10 wt% **Au-1** doped film, the 10 wt% **Au-1**:0.5 wt% **Au-7** co-doped film, and the 10 wt% **Au-1**:1 wt% **Au-7** co-doped film are 0.52, 0.22, and 0.16 μs, respectively.

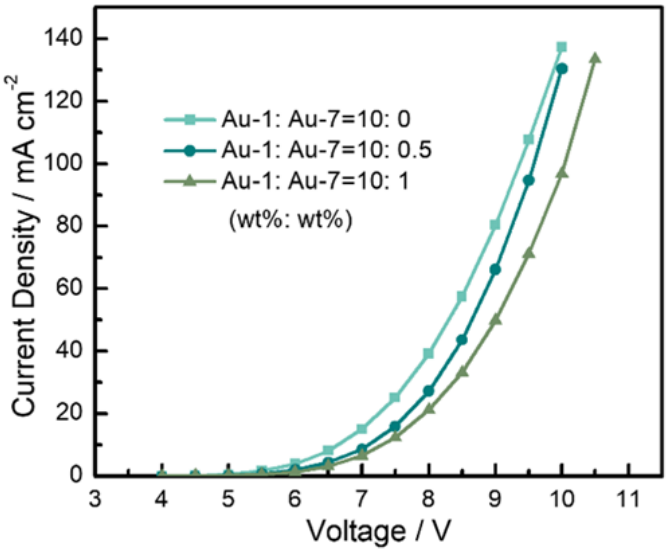

Figure S6. Current density−voltage characteristics of devices with different blend ratios of **Au-1** and **Au-7**.

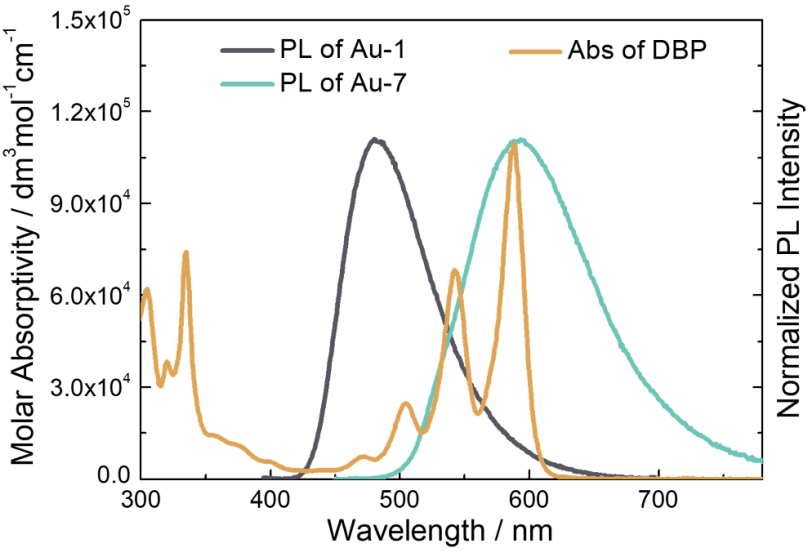

Figure S7. Absorption spectrum of DBP in toluene solution (2×10^{-5} mol dm^{-3}, orange line) and normalized emission spectra of **Au-1** (10 wt%, black line) and **Au-7** (10 wt%, green line) in PYD2 thin films. [The overlap of the emission spectrum of **Au-1** and the absorption spectrum of DBP gives a spectral integral $J(\lambda)$ of 1.34×10^{15} M^{-1} cm^{-1} nm^4, while the spectral overlap between **Au-7** and DBP affords a spectral integral $J(\lambda)$ of 4.12×10^{15} M^{-1} cm^{-1} nm^4.]

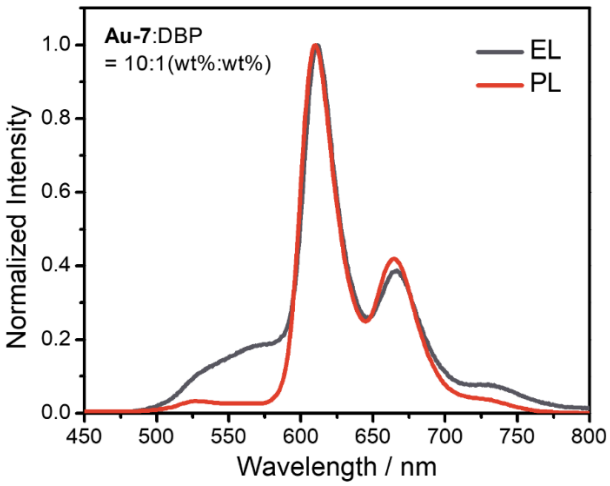

Figure S8. Normalized PL spectrum (red line) of the 10 wt% **Au-7**:1 wt% DBP co-doped film and normalized EL spectrum (black line) of the 10 wt% **Au-7**:1 wt% DBP-based device.

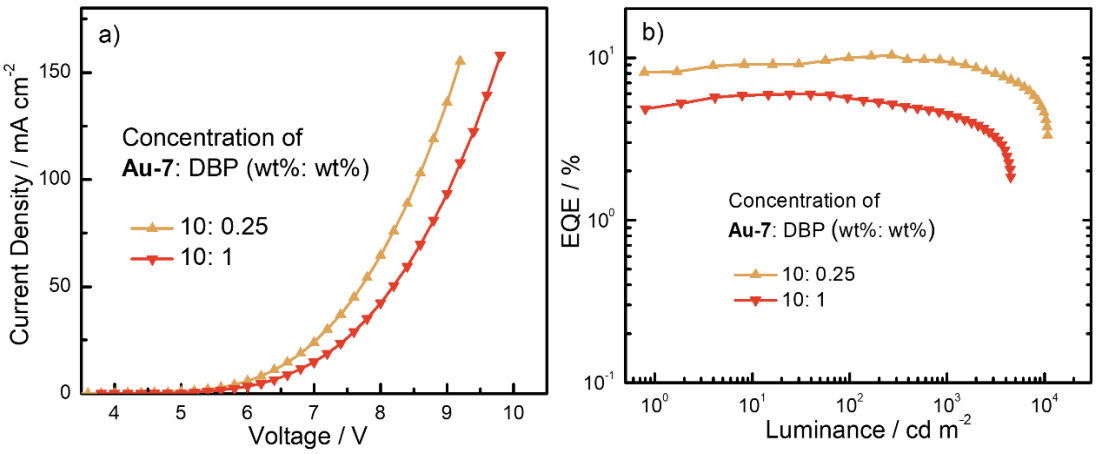

Figure S9. a) Current density−voltage b) EQE−luminance characteristics of OLEDs based on **Au-7** and DBP at different concentrations.

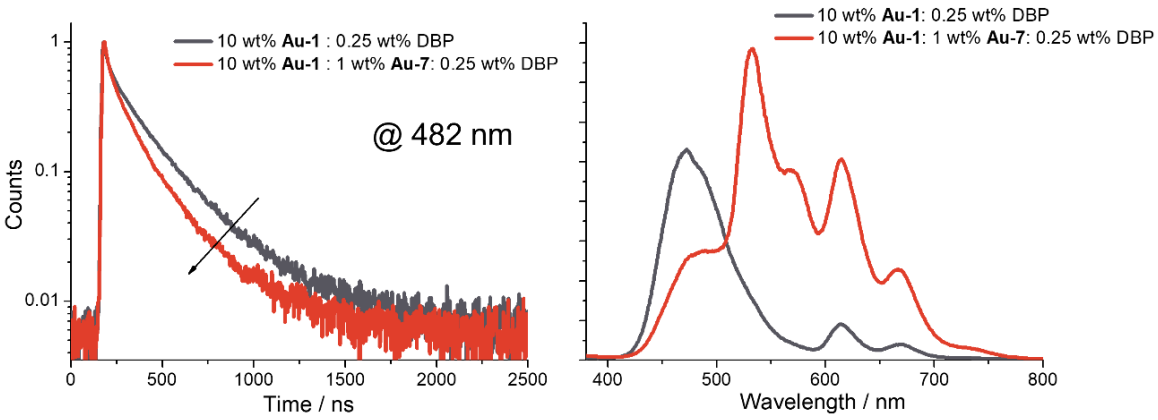

Figure S10. PL decay curves (left) and emission spectra (right) of the studied thin-film samples (the decay curves were measured at 482 nm under air). The weighted lifetimes of the 10 wt% **Au-1**:0.25 wt% DBP and 10 wt% **Au-1**:1 wt% **Au-7**:0.25 wt% DBP co-doped films are 0.19 and 0.14 μs, respectively.

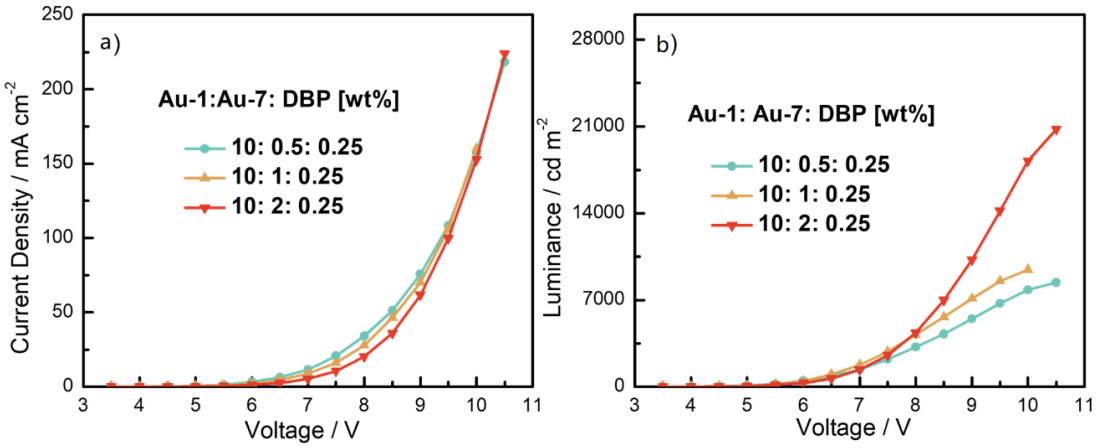

Figure S11. a) Current density−voltage and b) luminance−voltage characteristics of three-color WOLEDs based on **Au-1**, **Au-7**, and DBP at different doping concentrations.

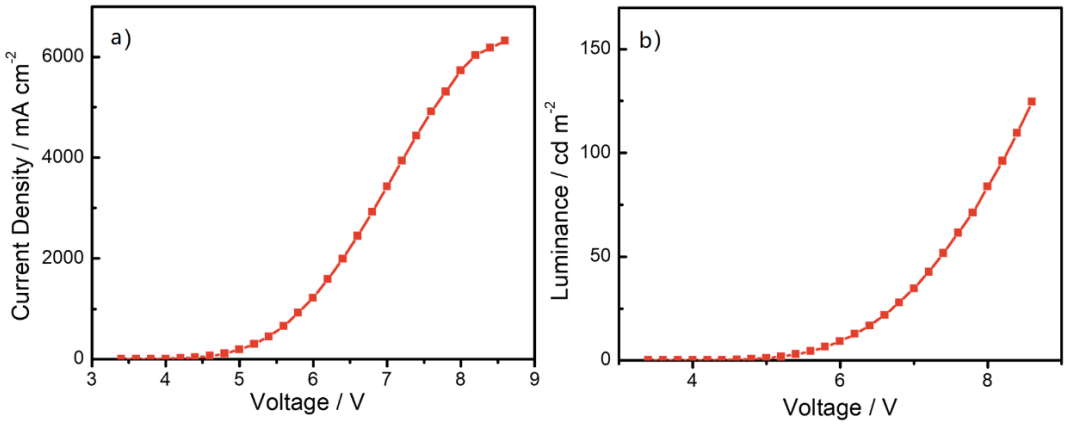

Figure S12. a) Current density−voltage and d) luminance−voltage characteristics of the three-color WOLED based on **Au-1** (10 wt%), **Au-8** (1 wt%), and DBP (0.25 wt%).

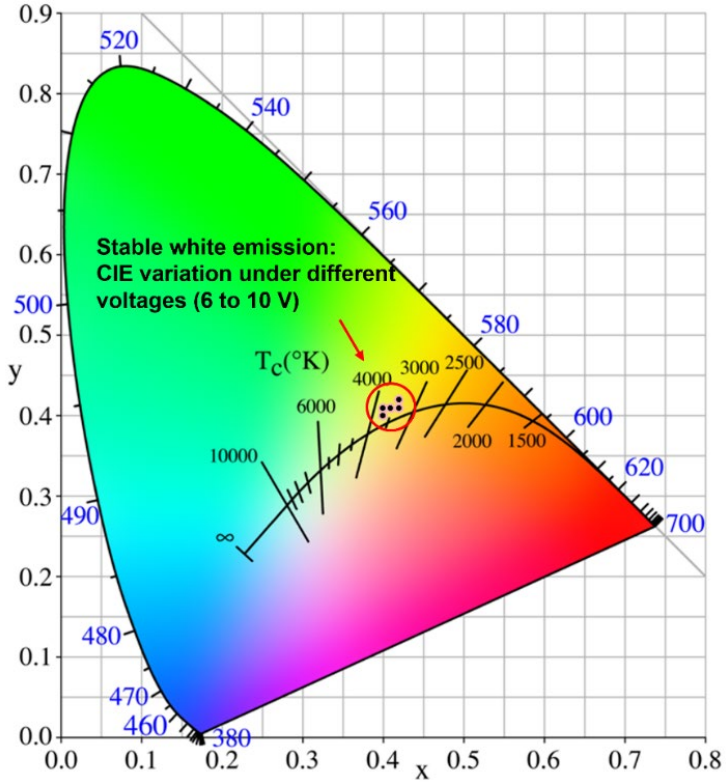

Figure S13. CIE Coordinates of the device based on **Au-1** (10 wt %), **Au-7** (1 wt%), and DBP (0.25 wt%) at different driving voltages (6−10 V).

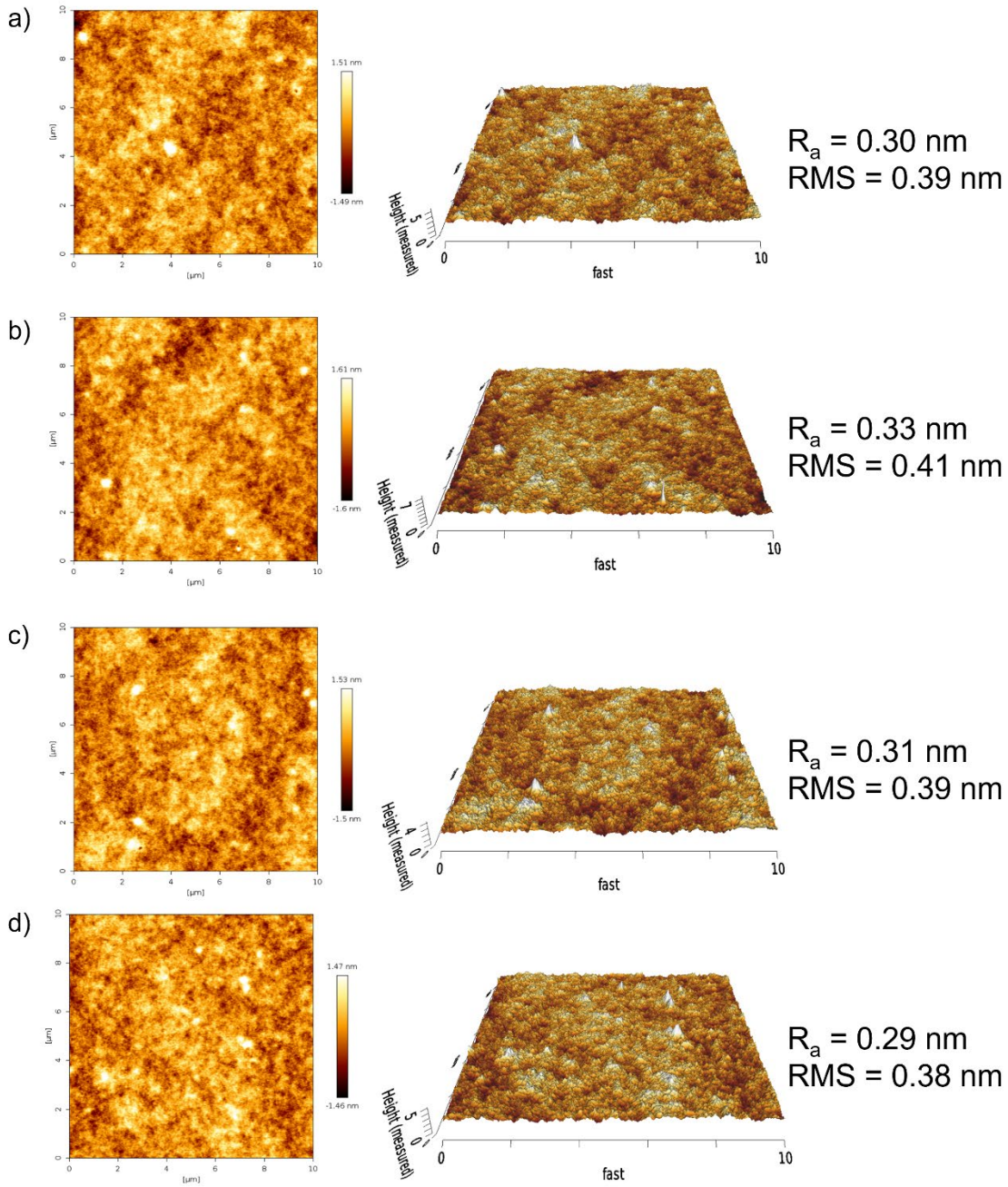

Figure S14. 2D and 3D AFM images (10×10 μm^2) of four PYD2 thin-film samples with corresponding R_a and RMS values: a) 10 wt% **Au-1**:0.5 wt% **Au-7**, b) 10 wt% **Au-1**:0.5 wt% **Au-8**, c) 10 wt% **Au-1**:1 wt% **Au-7**:0.25 wt% DBP, and d) 10 wt% **Au-1**:1 wt% **Au-8**:0.25 wt% DBP.

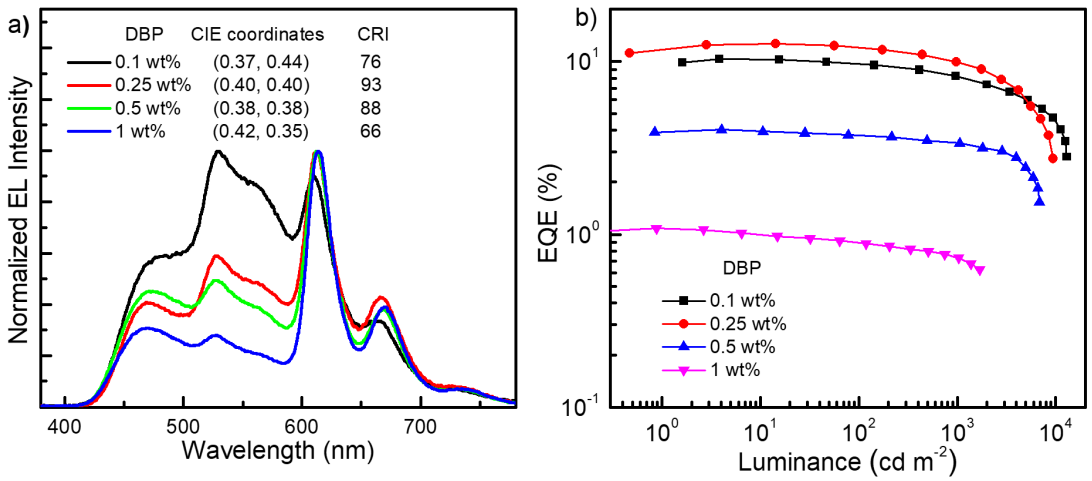

Figure S15. Optimization of WOLEDs based on **Au-1**, **Au-7**, and DBP. The doping concentrations of **Au-1** and **Au-7** were set to 10 wt% and 1 wt%, respectively, while the concentration of DBP ranged from 0.1 to 1 wt%. a) Normalized EL spectra and b) respective EQEs as a function of luminance of the studied three-component WOLEDs.

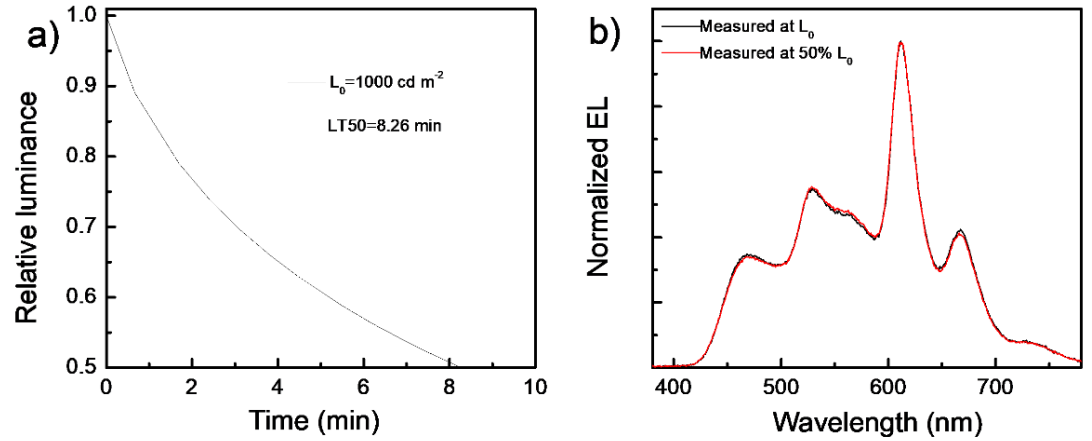

Figure S16. a) Relative luminance against operation time of the device based on **Au-1** (10 wt%), **Au-7** (1 wt%), and DBP (0.25 wt%) at an initial luminance (L_0) of 1000 cd m^{-2}; b) Normalized EL spectra of the WOLED before and after lifetime measurement.

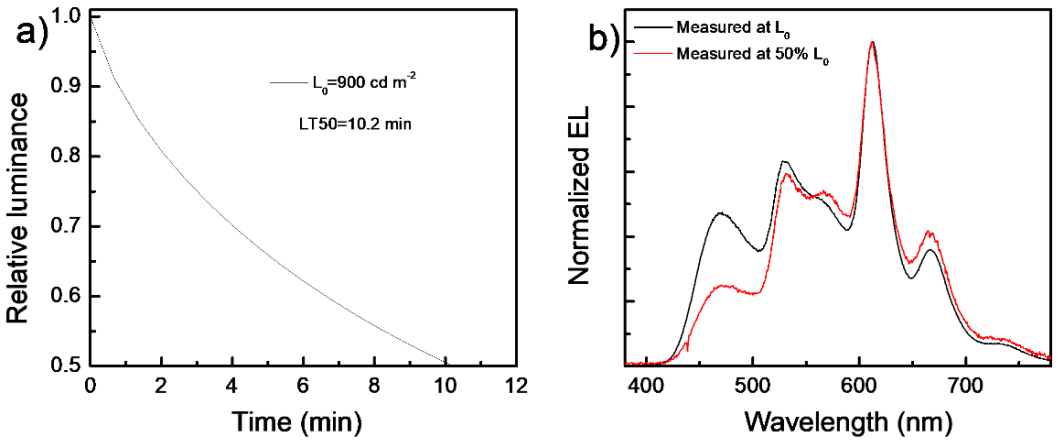

Figure S17. a) Relative luminance against operation time of the device based on **Au-1** (10 wt%), **Au-8** (1 wt%), and DBP (0.25 wt%) at an initial luminance (L_0) of 900 cd m^{-2}; b) Normalized EL spectra of the WOLED before and after lifetime measurement.

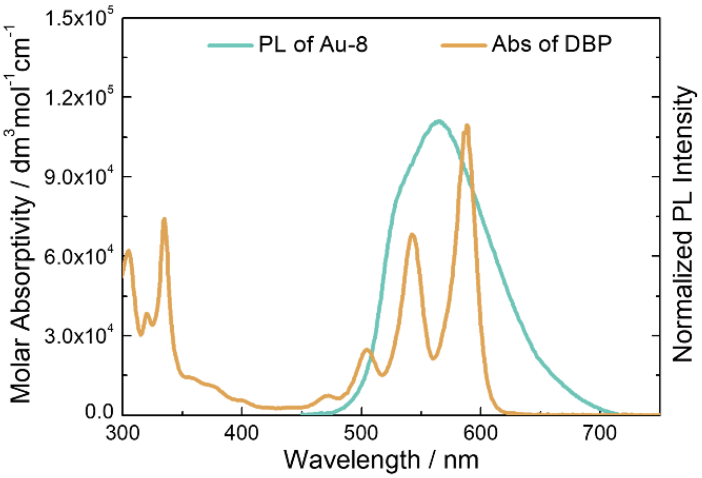

Figure S18. Absorption spectrum of DBP in toluene solution (2×10^{-5} mol dm^{-3}) and normalized emission spectrum of **Au-8** (10 wt% doped in the PYD2 host). [The overlap of the emission spectrum of **Au-8** and the absorption spectrum of DBP afforded a spectral integral $J(\lambda)$ of 3.67×10^{15} M^{-1} cm^{-1} nm^4, and accordingly, the R_{FRET} for **Au-8**/DBP was calculated to be 4.39 nm.]

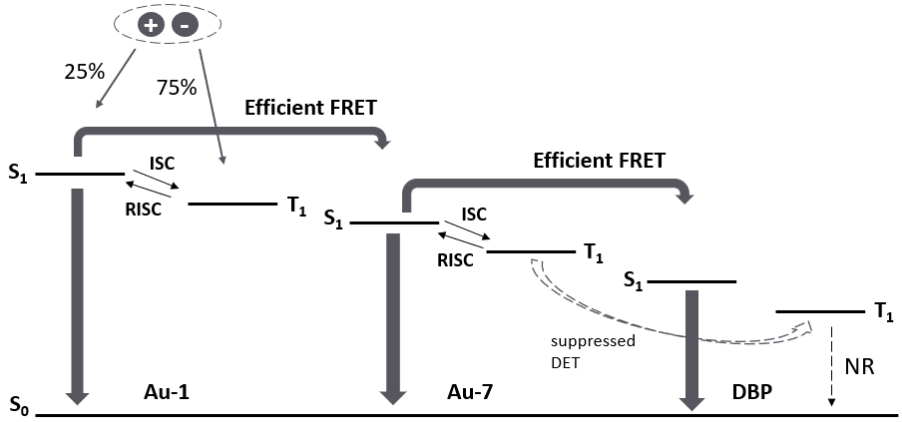

Figure S19. Proposed primary energy transfer and emission decay processes of the studied WOLEDs.

Table S1. Photophysical data of **Au-7** and **Au-8** doped in PYD2 thin films.

Emitter	λ_{em} [nm] [a)]	FWHM [nm; cm^{-1}]	Φ [%] [b)]	τ [μs] [b)]	$k_r \times 10^5$ [s^{-1}]
Au-7 (4 wt%)	573	119; 3514	71	0.95	7.45
Au-7 (10 wt%)	592	115; 3226	63	1.03	6.12
Au-8 (4 wt%)	532, 564	115; 3520	33	3.61, 0.28 [c)]	--
Au-8 (10 wt%)	532sh, 564	99; 3098	28	1.25	2.24

a) "sh" stands for shoulder; b) emission quantum yields (Φ) and emission lifetimes (τ) were measured under argon atmosphere; c) measured at 564 nm.

Table S2. Emission data of co-doping systems.

Co-doping system	λ_{em} [nm]	Φ [%]
Au-1(10 wt%):**Au-7**(0.5 wt%)	482, 528, 563	65
Au-1(10 wt%):**Au-7**(1 wt%)	482, 531, 562	57
Au-1(10 wt%):**Au-8**(0.5 wt%)	482, 528, 564	55
Au-1(10 wt%):**Au-8**(1 wt%)	482, 529, 564	38
Au-1(10 wt%):**Au-7**(1 wt%):DBP (0.25 wt%)	482, 532, 569, 615, 667	48
Au-1(10 wt%):**Au-8**(1 wt%):DBP (0.25 wt%)	482, 530, 568, 616, 667	33

Table S3. Key performances of single-EML SP-WOLEDs reported in this work and in the literature.

Device type	EQE (%)		CE_{max} (cd A^{-1}); PE_{max} (lm W^{-1})	CIE (x, y)	CRI	Ref.
	Max	At 1000 cd m^{-2}				
Two-color WOLED	17.84	16.45	49.78; 30.63	0.30, 0.40	71	**This Work**
Three-color WOLED	12.72	9.95	28.51; 22.28	0.40, 0.40	93	**This Work**
Two-color WOLED	20.8	11.8	N/A; 31.3	0.33, 0.39	76	4a
	12.32	N/A	28.8; 18.1	0.38, 0.44	67	4b
	23.51	N/A	N/A; 55.5	0.29, 0.36	71	4c
	22.57	N/A	37.27; 20.88	0.34, 0.35	73	4d
	15.0	N/A	40.0; 30.0	0.33, 0.44	< 70	4e
	26	16.4	70.6; 47.6	0.38, 0.43	62	4f
	12.73	11.51	27.44; 17.01	0.41, 0.45	74	4g
	10.02	N/A	21.10; 20.71	0.32, 0.33	85	4h
	11.93	N/A	30.76; 21.93	0.34, 0.43	75	4i
	11.5	N/A	29.3; 19.7	0.44, 0.38	70	4j
	14.2	N/A	38.8; 20.3	0.33, 0.42	70	4k
Three-/four-color WOLED	N/A	N/A	9.8; 8.9	0.36, 0.37	91	5a
	12.6	N/A	15.6; 10.4	0.36, 0.33	90	5b
	N/A	N/A	18.9; 9.6	0.45, 0.44	91	5c
	5.38	N/A	10.19; 6.10	0.35, 0.35	92	5d
	10.9	N/A	27.6; 16.4	0.38, 0.47	71	4e

Table S4. Key performances of vacuum-deposited WOLEDs with CRI ≥ 90 reported in the literature.

EQE_{max} [%]	CE_{max} [cd A^{-1}]	PE_{max} [lm W^{-1}]	CIE [x, y]	CRI	Ref.
6.5	N/A	9.0	0.46,0.45	90	12a
4.13	8.27	5.48	0.35,0.36	97	12b
4.14	8.78	5.63	0.32, 0.34	94	
10.3	24.0	16.4	0.32,0.35	94	12c
N/A	N/A	8.3	0.33,0.36	96	12d
N/A	N/A	23.3	0.43, 0.46	93	12e
N/A	N/A	N/A	0.32,0.34	91.2	12f
N/A	12.5	7.86	0.45, 0.40	96	12g
N/A	N/A	24.8	0.46,0.46	92	12h
N/A	N/A	5.5	0.49, 0.41	91.3	12i
15.6	23.1	20.6	0.54,0.42	95	12j
17.71	34.15	29.51	0.50,0.44	94	12k
N/A	9.52	11.08	0.25,0.26	93	12l
N/A	21.71	18.08	0.49,0.42	94	12m
14.20	13.37	12.92	0.55,0.38	95	12n

References:

[1] D. Zhou, G. Cheng, G. S. M. Tong, C.-M. Che, *Chem. Eur. J.* **2020**, *26*, 15718−15726.

[2] D. Zhou, W.-P. To, Y. Kwak, Y. Cho, G. Cheng, G. S. M. Tong, C.-M. Che, *Adv. Sci.* **2019**, *6*, 1802297.

[3] P. C. Wei, D. D. Zhang, L. Duan, *Adv. Funct. Mater.* **2020**, *30*, 1907083.